CrossMark

Research paper

Spatial turning bands simulation of anisotropic non-linear models of coregionalization with symmetric cross-covariances

D. Marcotte

Département des génies civil, géologique et des mines, Polytechnique Montréal, C.P. 6079 Succ. Centre-ville, Montréal, Qc, Canada H3C 3A7

ABSTRACT

The turning bands method (TBM) is a commonly used method of simulation for large Gaussian fields, its $O(N)$ complexity being unsurpassed (N denotes the number of points to simulate). TBM can be implemented either in the spatial or the spectral domains. In the multivariate anisotropic case, spatial versions of TBM are currently available only for the linear model of coregionalization (LMC). For anisotropic non-LMC with symmetrical covariances only the spectral version is currently available. The spectral domain approach can be slow in the case of non-differentiable covariances due to the numerous frequencies to sample. Here a derivation of the equations is provided for simulating the anisotropic non-LMC directly in the spatial domain and the method is illustrated with two synthetic examples. The approach allows the specification of many different direct and cross-covariance components, each with possibly different geometric anisotropies and different model types. The complexity of the new multivariate approach remains $O(N)$. Hence, a case of two variables defining an anisotropic non-LMC is simulated over one billion points in less than one hour on a desktop computer. These results help enlarge the scope of application of the TBM. The method can be easily implemented in any existing TBM program.

© 2016 Elsevier Ltd. All rights reserved.

1. Introduction

Most multivariate applications of geostatistics rely on the use of the linear model of coregionalization (LMC) (Journel and Huijbregts, 1978; Chilès and Delfiner, 2012; Wackernagel, 2003). However, in real applications the secondary variables are often of a different nature compared to the primary variable. As an example, geophysical variables like gravity or conductivity are representative of a larger (but unknown) support than the grade measured on cores and consequently they present a more continuous behavior at the origin. In these cases, the LMC cannot represent adequately the spatial joint variations of the variables. It has been shown (Marcotte, 2015) that estimation precision or simulation conditioning and realism can be improved significantly by using a suitable non-LMC compared to a forced LMC.

Two likely reasons for the nevertheless persistent popularity of the LMC are (1) the easy verification of the admissibility of the model and (2) the availability of simulation methods as LMC can be simulated by adding a set of univariate realizations. First, a sufficient (but not necessary) condition for the LMC to be admissible is that all coefficient matrices defining the LMC be positive semi-definite (Journel and Huijbregts, 1978; Goulard and

Voltz, 1992). In contrast, a non-LMC requires the verification that frequency dependent spectral matrices are positive semi-definite at every frequency, a challenging task. To help verifying this necessary and sufficient condition, Marcotte (2015) derived closed-form expressions of the spectral densities in the 3D anisotropic case for seven common covariance models. Marcotte (2015) also provided a simple program to implement these equations in a general context with multiple covariance components having possibly different anisotropies and model types on each component. Second, contrary to LMC, non-LMC requires the joint simulation of the variables. This can be achieved using spatial methods of Cholesky decomposition, a generalized version of the FFTMA approach (G-FFTMA), multivariate sequential Gaussian simulation (M-SGS) and continuous spectral methods (Shinozuka and Jan, 1972). The Cholesky approach is limited to small fields of only a few thousand nodes. The G-FFTMA has high memory requirements especially in 3D case where either the correlation ranges or the field to be simulated are large. M-SGS is known to be slow for large fields and to reproduce only approximately the desired covariances (Paravarzar et al., 2015) as it works with local neighborhoods.

A computationally less demanding alternative is the turning bands method (TBM) (Matheron, 1973; Journel and Huijbregts, 1978; Emery and Lantuéjoul, 2006). The multivariate case (M-TBM) has been developed by Mantoglou (1987) in the spectral

domain. The spectral version of M-TBM has the advantage of simplicity of the relation between the 3D spectral density and the 1D spectral density on the lines Mantoglou (1987). Using the 3D anisotropic spectral density expressions given in Marcotte (2015), it is straightforward to compute the line joint spectral densities for each anisotropic covariance component. Then, the 1D multivariate model can be simulated by a continuous spectral method (Shinozuka, 1971; Shinozuka and Jan, 1972). But, as remarked by Lantuéjoul (2002) and Chilès and Delfiner (2012), this amounts to simulate directly in 3D using the continuous spectral method, known to have slower convergence (Lantuéjoul, 1994, 2002), especially when the covariances are non-differentiable at the origin like the common spherical and exponential models. The use of importance sampling has been proposed recently Emery et al. (2016) to improve convergence of spectral TBM. Their method is flexible as it permits simulation of odd cross-covariances and the joint simulation of a variable and its regularization. To the author's knowledge, there is no M-TBM spatial version outside the restrictive LMC.

This paper extends the applicability of the spatial M-TBM method to the case of a more general anisotropic model allowing any number of different covariance components and anisotropies in the multivariate model. For simplicity, only the 3D stationary case is considered. Other restrictions are that each component of the cross-covariances should be symmetric and each component shows an anisotropy of the geometric type, i.e. the main correlation directions are the axes of an ellipsoid not necessarily parallel to the coordinate axes. The approach proceeds by determining the line joint covariances to simulate from the expressions for the line spectral densities using the relations presented in Mantoglou (1987) and Marcotte (2015) for the anisotropic case. Then the required line joint covariances can be simulated on each line in the spatial domain by any multivariate method, for example generalized G-FFTMA, Cholesky decomposition or M-SGS. The simulated values on each line are then combined as usual to get the 3D simulation at any desired simulation point.

After reviewing the theoretical background of spectral and spatial TBM, the 1D joint covariances for simulating along the lines are derived and synthetic examples are presented illustrating the capacity of the method to reproduce by TBM any combination of models with various anisotropies. Computational aspects are discussed.

2. Theoretical background

A stationary covariance function in $\Re^d$ has the spectral representation (Mantoglou, 1987; Lantuéjoul, 2002; Chilès and Delfiner, 2012):

$$C(h) = \int_{\Re^d} e^{i(s \cdot h)} F(ds) \tag{1}$$

where $\cdot$ is the inner product and $F(ds)$ is the spectral measure. When $C(h)$ is square integrable, the spectral measure can be written as a spectral density, $F(ds) = f(s)\,ds$. In 3D, the spectral density is given by (Lantuéjoul, 2002):

$$f_3(s) = \frac{1}{(2\pi)^3} \int_{\Re^3} C(h) e^{-i(s \cdot h)}\,dh \tag{2}$$

where $s = [s_x, s_y, s_z] = |s|u$, $|s|$ is the norm of vector s, $u = [u_x, u_y, u_z]$ is a unit vector parallel to s and h is the separation vector between two points.

Using spherical coordinates, and assuming (temporarily) that the anisotropy directions are parallel to the coordinate axes, the 3D anisotropic spectral density can be related to the 3D isotropic spectral density with range 1, by Marcotte (2015):

$$f_3(s) = a_g^3 f_{3,iso,a=1}(|s|b_u) \tag{3}$$

where $a_g^3 = a_x a_y a_z$ and $b_u = (a_x^2 u_x^2 + a_y^2 u_y^2 + a_z^2 u_z^2)^{1/2}$. Similarly, the 3D anisotropic spectral density $f_3(s)$ can also be expressed as a function of the 3D radial spectral density obtained with the same model and range b_u:

$$f_3(s) = \frac{a_g^3}{b_u^3} f_{3,iso,a=b_u}(|s|) \tag{4}$$

Mantoglou (1987) related the 3D spectral density to the 1D spectral density of the line covariance:

$$f_3(s) = f_{TB,u}(|s|)/(2\pi|s|^2) \tag{5}$$

Combining Eqs. (4) and (5) brings, for a particular direction u:

$$f_{TB,u}(|s|) = (2\pi|s|^2)\frac{a_g^3}{b_u^3} f_{3,iso,a=b_u}(|s|) \tag{6}$$

Taking the 1D Fourier transform on both sides of Eq (6) leads to:

$$C_{TB,u}(|h|) = \frac{a_g^3}{b_u^3} \frac{d}{dh} |h| C_{3,iso,a=b_u}(|h|) \tag{7}$$

In words, in the general anisotropic case, the TB covariance along the line of direction u is equal, up to the multiplicative factor $\frac{a_g^3}{b_u^3}$, to the TB line covariance obtained by applying the usual 3D *isotropic* inversion formula to the 3D-isotropic covariance of range b_u. This new result allows easy determination of the covariances to simulate along each line in the TBM so as to ensure the desired 3D anisotropy. The expressions are the same as for the isotropic case, except that the range b_u changes with direction u. This range is easily computed knowing the direction of line u with respect to the main axes of the ellipsoid. Note that when the axes of the ellipsoid are not parallel to the coordinate axes, it suffices to define the rotation matrix R that makes the coordinate axes parallel to the ellipsoid. Then the unit vectors v defining the directions in the original space are simply rotated in the same way, i.e. $u = vR$ and all computations apply to the rotated direction u. Therefore, the TBM can be applied as easily in the spatial domain as it was in the spectral domain in Mantoglou (1987). However, it is easier to simulate the required joint covariances in the spatial domain as simple methods such as SGS, G-FFTMA and Cholesky decomposition can be used.

It is worth noting that the range b_u does not define an ellipsoid when u sweeps the unit sphere. Rather, it is $1/b_u$ that defines an ellipsoid with main axes $1/a_x$, $1/a_y$, $1/a_z$ as shown in Fig. 1. Table 1 gives the covariances $C_{TB,u}(|h|)$ to simulate on lines u for 7 of the most common models. The list can easily be extended to include other models as well.

Note that in the univariate case it is usually faster to transform the domain to an isotropic one and simulate in the transformed space rather than to compute the anisotropic line covariance directly in the untransformed space with Eq (7). One Cholesky decomposition per anisotropic component will be needed in the first case, and one per line in the second instance. The real value of Eq. (7) is for the anisotropic non-LMC situation.

2.1. The multivariate case

The method generalizes to the anisotropic non-LMC with symmetrical cross-covariances. The line covariances and line cross-covariances are computed using the corresponding expressions listed in Table 1. Then the simulation is done *jointly* on the points discretizing each line. This step can be done using SGS, Cholesky, G-FFTMA or a continuous (Shinozuka, 1971; Shinozuka
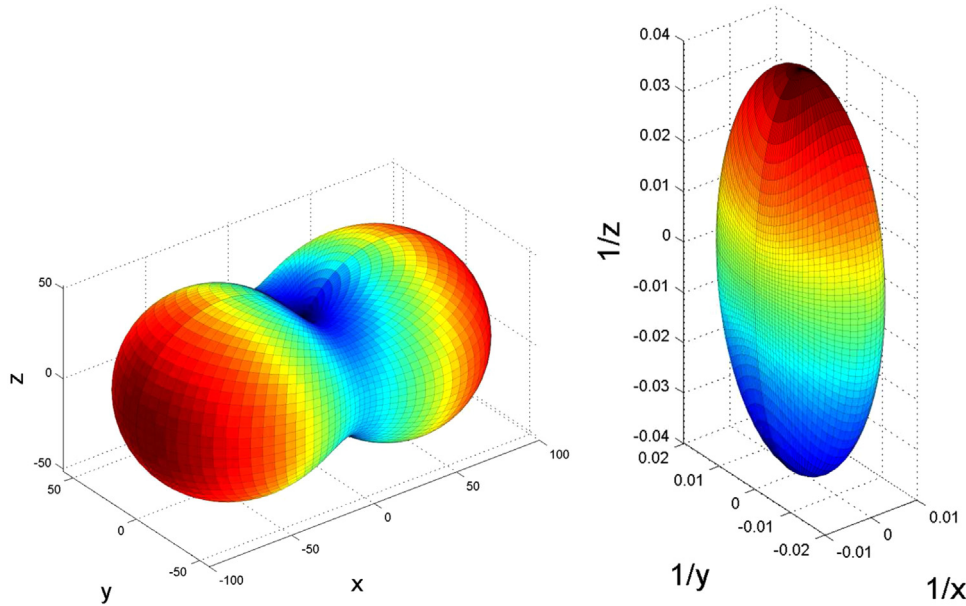
Fig. 1. Ranges b_u (left) and inverse of the ranges $1/b_u$ (right) as a function of direction defined by u.

and Jan, 1972; Mantoglou, 1987) spectral method or any suitable 1D method allowing multivariate joint simulation. Note that the discretization along the lines (needed for G-FFTMA) introduces an error that was shown to be negligible when more than 20 discretization points per correlation length were used on each line for cases with only 16 lines (Mantoglou and Wilson, 1982) and 81 lines (Freulon and de Fouquet, 1991). For multi-component covariances and cross-covariances, contributions of each of the components are added on each line prior to the line simulation. Discretization along the lines can be avoided by using continuous methods of simulation (Lantuéjoul, 1994, 2002) (e.g. with the continuous spectral method or SGS). However the number N of points to simulate is usually orders of magnitudes larger than the number n of discretization points along the lines, which makes simulation more CPU intensive.

The 3D multivariate model is admissible if and only if all line multivariate models are admissible. This result stems from the relation between spectral matrices in $\Re^3$ ($\tilde{f}_3(\cdot)$) and those of the lines of the TBM ($\tilde{f}_{TB,u}(\cdot)$) (Mantoglou, 1987):

$$\tilde{f}_{TB,u}(|s|) = 2\pi|s|^2 \tilde{f}_3(|s|u) \tag{8}$$

where $|s|$ is the scalar frequency along the line defined by the unit vector u, $\tilde{f}_{TB,u}(|s|)$ is the spectral matrix associated with line u at frequency $|s|$ in the TBM and $\tilde{f}_3(|s|u)$ is the spectral matrix in the 3D

space at frequency vector $|s|u$. As $2\pi|s|^2$ is positive, a negative eigenvalue of $\tilde{f}_{TB,u}(|s|)$ at any $|s|$ implies a negative eigenvalue on $\tilde{f}_3(|s|u)$ at the frequency vector $|s|u$ and vice versa.

Different types of models with different ranges and rotations or anisotropy ratios can be specified for each covariance and cross-covariance component. It is then however necessary to verify the admissibility of the 3D model (or equivalently all line models). For this, a program like TASC3D (Marcotte, 2015) can be useful.

3. Computational aspects

The complexity of the algorithm in terms of multiplications and divisions is described (additions are neglected). Assume that N points are to be simulated by TBM for p correlated variables and k realizations, using L lines and n discretization points on each line. For simplicity here, the simulation on each line is done using a Cholesky method. The complexity of the usual Cholesky decomposition is $O(n^3p^3)$ for one line. Taking advantage of the Toeplitz structure of the line covariance matrix defined by discretization points reduces the complexity to $O(n^2p^2)$ (Dietrich, 1993). Generating the k realizations on each line requires $O(kn^2p^2)$. So, this step is $O(L(kn^2p^2))$. Then, the N points are projected on each of the L lines giving a complexity of $O(NL)$ (the p ensuing additions are neglected). Usually one has $N \gg n \gg p$, so the global complexity for

Table 1

Line turning bands covariance of some common 3D anisotropic covariance functions; $h_u = |h|/b_u$, $C_u = C\frac{a_g^3}{b_u^3}$, $a_g = (a_x a_y a_z)^{1/3}$, $b_u = (a_x^2 u_x^2 + a_y^2 u_y^2 + a_z^2 u_z^2)^{1/2}$, $u = [u_x, u_y, u_z]$ is the unit vector defining the line and $I(h_u) = 1$ when $|h| < b_u$, 0 otherwise.

Model	Definition $C_{3,iso,a=b_u}(h_u)$	TBM covariance $C_{TB,u}(|h_u|) = \frac{d}{dh_u}h_u C_{3,iso,a=b_u}(h_u)$
Exponential	$C(\exp(-h_u))$	$C_u \exp(-h_u)(1 - h_u)$
Gaussian	$C(\exp(-(h_u)^2))$	$C_u \exp(-(h_u)^2)(1 - 2(h_u)^2)$
Spherical	$C(1 - 1.5h_u + 0.5(h_u)^3)I(h_u)$	$C_u(1 - 3(h_u) + 2(h_u)^3)I(h_u)$
Cubic	$C(1 - 7h_u^2 + \frac{35}{4}h_u^3 - \frac{7}{2}h_u^5 + \frac{3}{4}h_u^7)I(h_u)$	$C_u(1 - 21h_u^2 + 35h_u^3 - 21h_u^5 + 6h_u^7)I(h_u)$
Penta	$C(1 - \frac{22}{3}h_u^2 + 33h_u^4 - \frac{77}{2}h_u^5 + \frac{33}{2}h_u^7 - \frac{11}{2}h_u^9 + \frac{5}{6}h_u^{11})I(h_u)$	$C_u(1 - 22h_u^2 + 165h_u^4 - 231h_u^5 + 132h_u^7 - 55h_u^9 + 10h_u^{11})I(h_u)$
Cauchy	$C(1 + h_u^2)^{-\alpha}$ with $\alpha > 0$	$C_u(1 - h_u^2 + 2\alpha h_u^2)/(1 - h_u^2)^{1+\alpha}$
K-Bessel (Matern)	$\frac{C}{2^{\nu-1}\Gamma(\nu)}h_u^\nu K_\nu(h_u)$ with $\nu \geq 0$	$\frac{C_u}{2^{\nu-1}\Gamma(\nu)}h_u^\nu (K_\nu(h_u) - h_u K_{\nu-1}(h_u))$

large fields is $O(NL)$. To give orders or magnitude, n and L are typically a few hundred, k is usually less than 100, p is a few units (often two or three) but N can easily reach 10^6–10^9.

Note that Mantoglou (1987) reports CPU times proportional to $N^{1/3}$ for the 3D case. However, only small fields ($N < 10^4$) were considered in this paper, so the dominant term was likely the line term. The spectral line method used to simulate discretization points was proportional to n as the number of frequencies was fixed to a small value. As the number of discretization points n was taken proportional to $N^{1/3}$, one gets the $N^{1/3}$ proportionality. For larger fields, the $O(NL)$ proportionality mentioned above would be observed.

The $O(NL)$ complexity is obtained when the same set of lines is used for each realization. Freulon and de Fouquet (1991) recommended to instead generate anew the set of lines for each realization to ensure overall better model reproduction. This increases the complexity to $O(kNL)$. Whether or not the gain in model reproduction worth the additional computations depends probably on the number of lines and the uniformity of their distribution on the sphere. With many lines (say $L > 500$) selected according to the Van der Corput sequence (Freulon and de Fouquet, 1991) so as to provide a uniform coverage, it is unlikely that taking a different sets of lines for each realization would improve substantially the model approximation. However, this remains to be proved formally.

Fig. 2 shows the execution time for a single realization of the bivariate non-LMC described in Table 3. The TBM operates with 100 lines each discretized by 100 points. Cholesky factorization is employed to simulate line joint covariances. As anticipated, one observes the proportional increase of execution time with N at large N values.

4. Examples

Two illustrative examples are examined. The first one is the univariate simulation of an anisotropic field. The second one is the simulation of a non-LMC anisotropic field. The direct and cross-variograms are computed and checked for reproduction of the theoretical ones. The variogram mean and standard deviation are computed over k realizations and the distribution of deviations of the mean variogram from the theoretical model are compared at each lag to a Student distribution as suggested in Emery (2008)
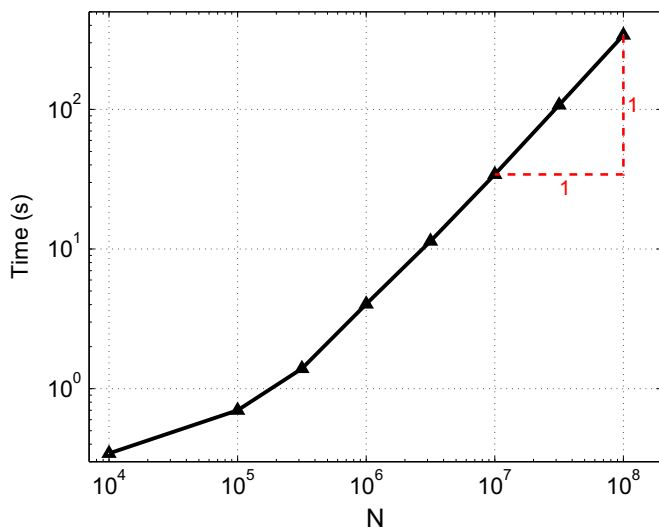
Table 2
Simulation parameters.

Simulation parameter	Symbol	Value
Number of points to simulate	N	10 000 (100 × 100)
Number of realizations	k	100
Number of lines	L	500
Number of discretization points on lines	n	500

and Paravarzar et al. (2015):

$$Z(h) = (\overline{\gamma_e}(h) - \gamma_{th}(h))/S_{\overline{\gamma_e}(h)} \tag{9}$$

with

$$\overline{\gamma_e}(h) = 1/k \sum_{i=1}^{k} \gamma_{e,i}(h) \tag{10}$$

$$S_{\overline{\gamma_e}(h)} = \frac{1}{\sqrt{k}} \left(\frac{1}{k-1} \sum_{i=1}^{k} (\gamma_{e,i}(h) - \overline{\gamma_e}(h))^2 \right)^{1/2} \tag{11}$$

4.1. Univariate anisotropic case

The 2D anisotropic fields are generated on a regular grid using the 3D TBM with the simulation parameters described in Table 2. The lines were uniformly distributed on the sphere using the Van der Corput sequence as suggested by Freulon and de Fouquet (1991) (Fig. 3). The same set of lines was used for each realization of a given run. When more than one run was used, a different set of lines was taken for each run. All variograms were computed using the FFT approach described in Marcotte (1996). Table 3 shows the models used.

Fig. 4 shows the individual realizations and the mean variogram obtained with the first model of Table 3. The 95% confidence interval for the mean variogram is also illustrated. The mean variogram is close to the theoretical one and the confidence interval around the theoretical model includes the mean variogram.
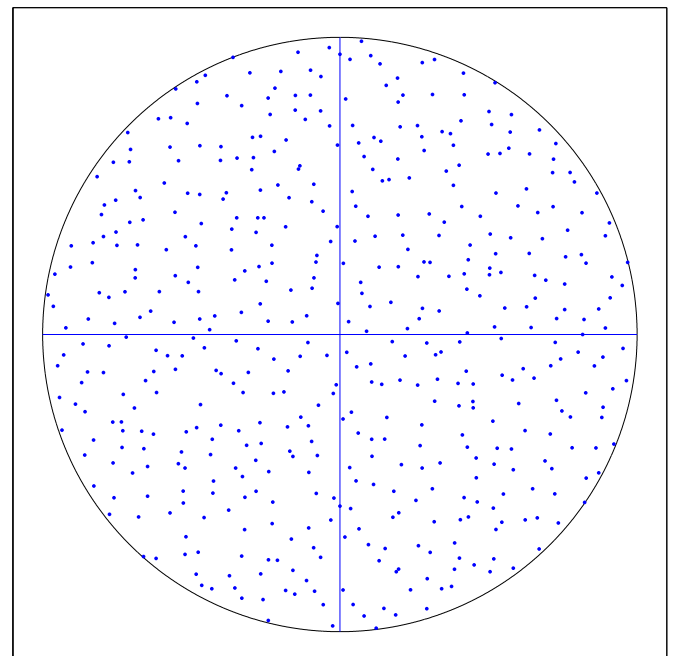

Fig. 2. Computation time vs. number of simulation points N; single realization; TBM with 100 lines, 100 discretization points per line.

Fig. 3. Five hundred lines obtained using the Van der Corput sequence represented on an equal area (Lambert azimuthal) projection.

Table 3
Description of the models.

Figure	Description	Model parameters
Fig. 4	Univariate	Spherical ($a_x = 40, a_y = 10, a_z = 10; C = 1$)
Fig. 6	Bivariate non-LMC	
	v1–v1	Matern ($a_x = a_y = a_z = 10; C = 1; \nu = 1$)
	v1–v2	Matern ($a_x = 15, a_y = 8, a_z = 10; C = 0.6; \nu = 1.6$)
	v2–v2	Matern ($a_x = 15, a_y = 6, a_z = 10; C = 1; \nu = 2$)

However, as the variogram values at different lags are correlated, runs with another random seed and the same number of realizations sometimes lead to a mean variogram almost systematically below or above the confidence interval. To assess the unbiasedness of the TBM implementation, 100 independent runs of 50 realizations each were realized. For each run, the proportion (over all lags) of mean variogram values outside the confidence interval was computed for various confidence levels. For a given confidence level, an empirical distribution of 100 proportions is therefore obtained. The mean and the first and third quartiles of these distributions are shown in Fig. 5. The confidence band of the PP-plot clearly includes the line of equality and the mean is almost superposed to this line. One can therefore conclude that no significant bias is present in the spatial anisotropic TBM implementation for this model and the choice of simulation parameters given in Table 2.

4.2. A non-LMC

The second model of Table 3 is a non-LMC bivariate model as the shape parameters and the ranges are different for the two direct covariances and the cross-covariance. The model admissibility was tested with program TASC3D (Marcotte, 2015). Fig. 6 shows the direct and cross-variograms obtained for the 50 realizations, the mean variogram, the theoretical model and the confidence intervals along x and y directions for a single run. The mean variogram is well within the confidence band around the theoretical model.

5. Discussion

The turning bands method is particularly appropriate to simulate large fields. First, its complexity is only $O(N)$ for a fixed number of lines and realizations. This is better than common methods like FFTMA, Cholesky, and SGS. Second, points can be
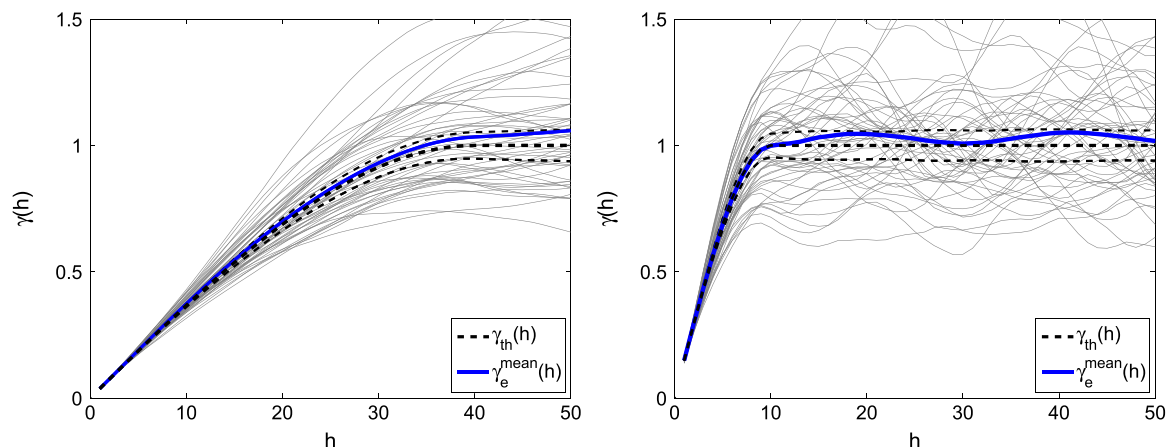
Fig. 5. PP-plot of mean variogram empirical CDF vs. Student distribution; 50 realizations; the solid line is the mean CDF over 100 repetitions; dashed lines are the first and third quartiles of the 100 runs.

simulated anywhere and according to any sequence. Hence, it is possible to simulate blocks without having to store the point simulation over the whole field. Third, the memory requirement of the method is not a problem as only the covariances along the lines, evaluated at chosen discretization points, need to be stored. This is in contrast to G-FFTMA, where available memory limits the size of the fields in 2D and 3D that can be simulated, or with SGS which needs to work locally to keep memory and CPU requirements to a reasonable level.

In the univariate case, the spatial implementation of TBM was in the past limited to isotropic univariate models or to geometric anisotropies where an affine correction on the coordinates enables the transformation of the field to an isotropic one. When the covariance is composed of multiple components with different geometric anisotropies, it is required to simulate separately each component and then add the different simulated components.

In the multivariate case, a similar spatial approach can be followed only when the LMC applies. It suffices to simulate each covariance component after suitable affine transformation to an isotropic field and then add the contributions linearly with weights computed from each coefficient matrix. However, in the non-LMC case, this approach is no more feasible as the variables must be simulated jointly to ensure the reproduction of all direct

Fig. 4. Variograms along x (left) and y (right) obtained for the different realizations; mean variogram (solid line), theoretical variogram and 95% confidence interval for the mean variogram (dashed lines).
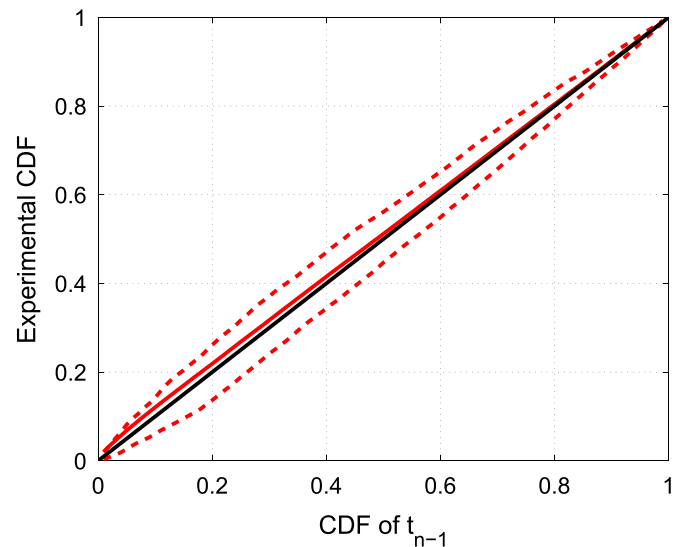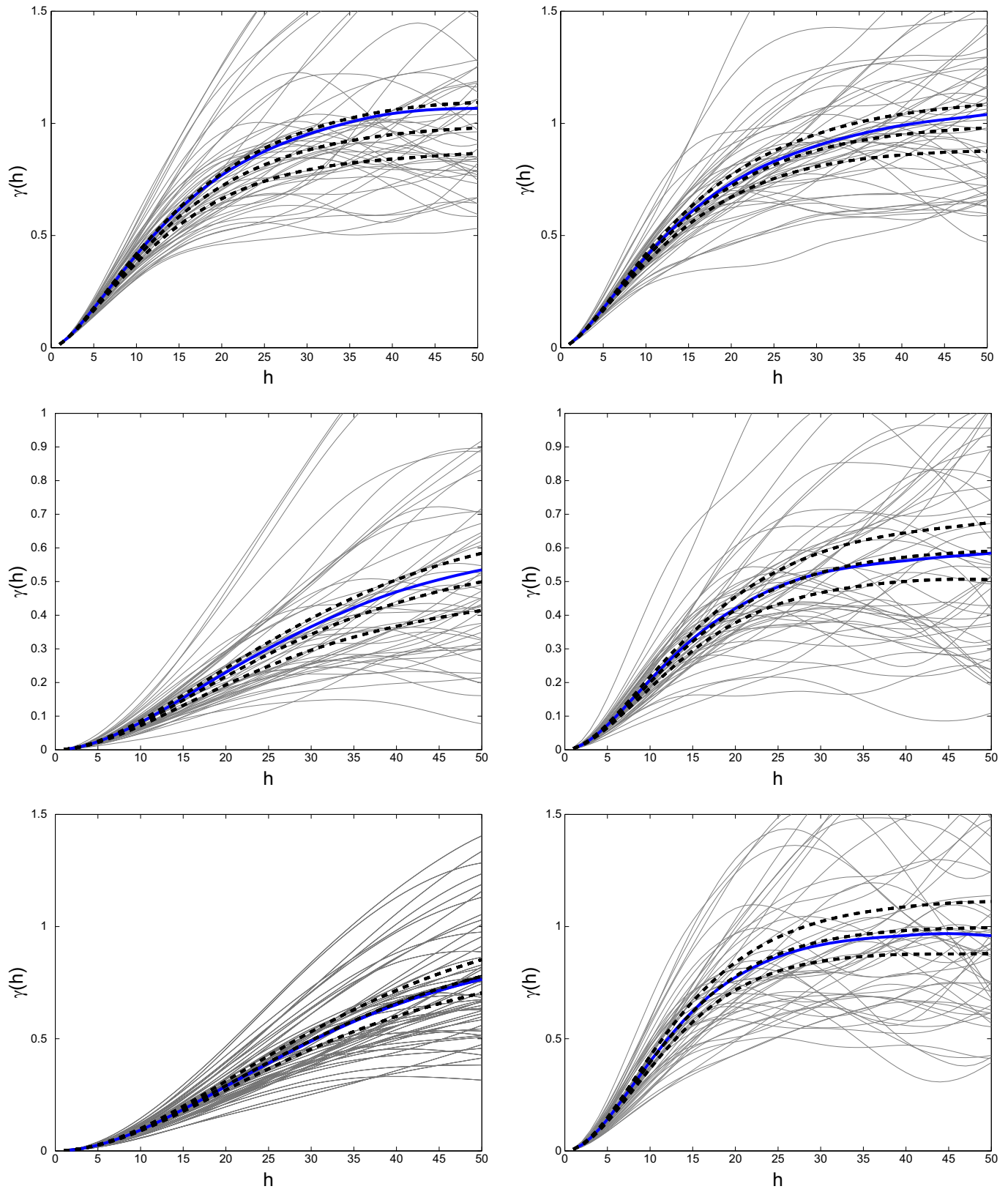
Fig. 6. Direct (first and third rows) and cross-variograms (middle row) along *x* (left column) and *y* (right column) obtained for 50 different realizations, non-LMC; mean variogram (solid line), theoretical variogram and 95% confidence interval for the mean variogram (dashed lines) are also shown.

and cross-covariances. The joint simulation can be done with the spectral approach (Mantoglou, 1987), but this can be slow when simulating non-differentiable covariances (Lantuéjoul, 1994, 2002; Chilès and Delfiner, 2012). In these cases, the spectral density decays slowly with the frequency, requiring the consideration of many frequencies in the simulation. Moreover, the spectral approach requires the decomposition (by Cholesky or eigendecomposition) of spectral matrices at all sampled frequencies. On

the other hand, the spatial approach developed in this paper enables straightforward simulation along each line with routinely available methods like Cholesky decomposition, multivariate SGS or G-FFTMA. It was illustrated, with a synthetic example, that the method is unbiased and reproduces the desired anisotropies. Asymptotically, as the number of lines and discretization points increase, the method is exact.

In the proposed spatial M-TBM, the covariances to simulate along each line are obtained by applying, separately to each component, the classic TBM inversion formula for a 3D isotropic model with range and scale factor computed according to the direction of the line. Hence, the covariance to simulate is line orientation dependent, similarly to the spectral approach where the line spectral density is also a function of the line orientation. Because of this dependence on line orientation, a different Cholesky decomposition (or other method) has to be done for each line. Nevertheless, Fig. 2 shows that the proposed method can simulate two correlated variables for up to one billion points in less than one hour (on an Intel Xeon), and this, without any parallelization.

Note that for the univariate case and the LMC, the current approach of affine correction is still to be preferred to the new method described. A single Cholesky decomposition per component needs to be done in contrast to one decomposition per line in the new approach. However, for non-LMC, only the new approach can be used in the spatial domain. The non-LMC considered assumes that all the cross-covariances are symmetric and that a valid non-LMC is specified. Lack of admissibility will eventually be detected by failure of the Cholesky line covariance decomposition.

Only the unconditional case was considered. The conditioning of the realizations to observed data can be done routinely by post-conditioning by cokriging (Chilès and Delfiner, 2012), using the same non-LMC. When the number of data does not exceed say 10 000, it is possible to do the conditioning quickly by using the dual formalism of kriging (Davis and Grivet, 1984; Royer and Vieira, 1984). The complexity of this operation is $O(mN)$ where m is the number of data. For a fixed number of data, the complexity remains $O(N)$ like for the unconditional simulation.

6. Conclusion

A spatial multivariate turning bands method was presented that allows us to simulate anisotropic non-LMC directly in the spatial domain. The expressions to use along each line were derived for seven of the most common covariance models. The covariance expressions along the lines are the same as in the classical 3D isotropic case, except that the range and the scale factor have to be computed as functions of the line direction. It was shown that the method is unbiased and fast. It provides a useful tool for the simulation of very large fields where other simulation method face CPU and memory restrictions. The proposed method can be easily included in any existing spatial TBM program.

References

Chilès, J., Delfiner, P., April 2012. Geostatistics: Modeling Spatial Uncertainty, 2nd ed. John Wiley & Sons, Hoboken, New Jersey.

Davis, M., Grivet, C., 1984. Kriging in a global neighborhood. Math. Geol. 16 (3), 149–265.

Dietrich, C.R., 1993. Computationally efficient Cholesky factorization of a covariance matrix with block Toeplitz structure. J. Stat. Comput. Simul. 45, 203–218.

Emery, X., 2008. Statistical tests for validating geostatistical simulation algorithms. Comput. Geosci. 34 (11), 1610–1620.

Emery, X., Arroyo, D., Porcu, E., 2016. An improved spectral turning-bands algorithm for simulating stationary vector Gaussian random fields. Stochast. Environ. Res. Risk Assess. Available at: DOI http://dx.doi.org/10.1007/s00477-015-1151-0.

Emery, X., Lantuéjoul, C., 2006. TBSIM: a computer program for conditional simulation of three-dimensional Gaussian random fields via the turning bands method. Comput. Geosci. 32 (10), 1615–1628.

Freulon, X., de Fouquet, C., June 1991. Remarques sur la pratique des bandes tournantes à 3D. In: Compte-rendu des journées de géostatistique, ser. Cahier de géostatistique, Fascicule 1, pp. 101–117.

Goulard, M., Voltz, M., 1992. Linear coregionalization model: tools for estimation and choice of cross-variogram matrix. Math. Geol. 24, 269–286.

Journel, A.G., Huijbregts, C.J., 1978. Mining Geostatistics. Academic Press.

Lantuéjoul, C., 1994. Non conditional simulation of stationary isotropic multi-Gaussian random functions. In: Armstrong, M., Dowd, P. (Eds.), Geostatistical Simulations, pp. 147–177.

Lantuéjoul, C., 2002. Geostatistical Simulation: Models and Algorithms. Springer, Berlin.

Mantoglou, A., 1987. Digital simulation of multivariate two- and three-dimensional stochastic processes with a spectral turning bands method. Math. Geol. 19 (February (2)), 129–149.

Mantoglou, A., Wilson, J.L., 1982. The turning bands method for simulation of random fields using line generation by a spectral method. Water Resour. Res. 18 (October (5)), 1379–1394.

Marcotte, D., 2015. TASC3D: A program to test the admissibility in 3D of non-linear models of coregionalization. Comput. Geosci. 83, 168–175.

Marcotte, D., 1996. Fast variogram computation with FFT. Comput. Geosci. 22 (10), 1175–1186.

Matheron, G., 1973. The intrinsic random functions and their applications. Adv. Appl. Probab. 5 (3), 439–468.

Paravarzar, S., Emery, X., Madani, N., 2015. Comparing sequential Gaussian and turning bands algorithms for cosimulating grades in multi-element deposits. C. R. Geosci. 347, 84–93.

Royer, J.-J., Vieira, P., 1984. Dual formalism of kriging. In: Verly, G., David, M., Journel, A.G., Maréchal, A. (Eds.), Geostatistics for Natural Resources Characterization, NATO-ASI 122, series C, pp. 621–634.

Shinozuka, M., 1971. Simulation of multivariate and multidimensional random processes. J. Acoust. Soc. Am. 49, 357–367.

Shinozuka, M., Jan, C.M., 1972. Digital simulation of random processes and its applications. J. Sound Vib. 25, 111–128.

Wackernagel, H., 2003. Multivariate Geostatistics: An Introduction with Applications, 3rd ed. Springer, Berlin.